RSC Advances

ROYAL SOCIETY OF CHEMISTRY

www.rsc.org/advances

Graphical abstract

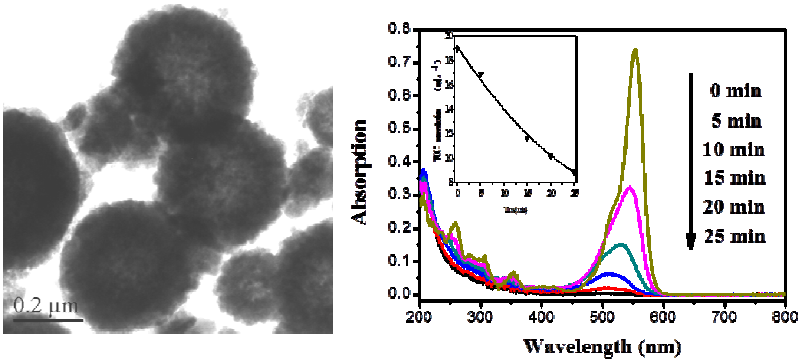

Hydrothermal Synthesis of Mn-Doped CdS Hollow Spheres Nanocomposite as Efficient Visible-Light Driven Photocatalysts

Chunyan Zhang[a,b], Jiasheng Lai[c], Juncheng Hu[a*]

[a]Key Laboratory of Catalysis and Materials Science of the State Ethnic Affairs Commission & Ministry of Education, South-Central University for Nationalities, Wuhan 430074, PR China
Email: junchenghuhu@hotmail.com
[b]Department of Chemistry and Life Science, Liuzhou Teachers College, Liuzhou 545004, PR China
[c]Department of Physics and Information Science, Liuzhou Teachers College, Liuzhou 545004, PR China

ABSTRACT

A series of Mn-doped CdS hollow spheres photocatalysts have been directly synthesized by a simple and facile hydrothermal route for the first time. It was demonstrated that GSH act as the S source and a gas bubble-template in this progress. The products were characterized by XRD, SEM, TEM, HRTEM, XPS, and UV-vis. The as-prepared CdS and Mn-doped CdS hollow spheres all showed much higher activity than P25 under visible light (λ>420 nm) irradiation. Among them, the 2.0 mol% Mn-doped CdS sample exhibited the highest photoactivity for the remove of organic pollutants RhB, and about 99.2 % MO was decomposed after 50 min visible light irradiation. Moreover, this catalyst also showed good stability, and after four recycles, the degradation efficiency still remained at 85 %. The excellent photoactivity of the as-prepared Mn-doped CdS hollow spheres could be attributed to a synergistic effect of its appropriate band-gap structure and the special porous spherical morphology. The unique hollow spheres structure may be favor of harvesting the exciting light due to its special multiple scattering effect within the interior space, and the doping of Mn^{2+} may facilitate the generation of photoinduced electrons and holes pairs and inhibit their recombination rate by acting as temporary trapping sites. This material may have great application potential in environmental remediation and energy harvest.

KEYWORDS: Hollow Spheres, CdS, doping, manganese, Photocatalysis

1. Introduction

Solar energy, due to its distinct advantages of clean, accessible and inexhaustible,[1] is being intensively pursued, especially the visible light portion which accounts for 43 % of the solar is attracting increasing attention.[2] Recently, the development of photocatalysts with high visible-light activities has

became a challenging and interesting topic. These photocatalysts can utilize abundant solar energy and water resources in nature to solve many related problems, such as organic pollutants degradation and H_2 production from water splitting.[3-5] the development of photocatalysts has become a challenging and interesting topic of research. Various approaches have been developed to enhance the activity and extend the response of photocatalysts to the visible light region, such as controlling the size and shape of nanocrystals. Because of the high light-harvesting efficiency, fast mobility of charge carriers, and superior catalytic activity,[6,7] hollow structured materials have been recognized as one type of promising material for applications in the field of photocatalytic processes. Man Luo et. al.[8] have prepared the general strategy for one-pot synthesis of metal sulfide hollow spheres. On the other hand, doping metallic (Pt, Au and Ag et. al.) and nonmetallic (C, N and F et. al.) elements into conventional photocatalysts to decrease the band gap is a very good choice .[9-15]

CdS, as an important II-VI group semiconductor material and a well-known visible-light-sensitive material,[16] with a band-gap of 2.42 eV, has attracted considerable attention for the conversion of solar energy into chemical energy in recent years. Lee and Shen[17] have reported kinds of CdS with various structures such as flowerlike nanostructures, tetrapod-like nanoorods and long branched NPs. However, the low separation efficiency of photogenerated electrons and holes and the fact that easily corroded making it not favorable for the wide applications in environmental remediation and solar conversion.[18,19] Recently, many studies that attempting to improve CdS photocatalytic performance focus on structure design or surface modification,[20-25] Such as nanowires, nanobelts, nanorods, and nanospheres. But it was not satisfying the achievement for increasing both the photoactivity and stability.[26-29] Metal ions doping (such as Mn, Co, Fe, Ni, etc.) is demonstrated to been an effective means in controlling the band gap and absorption properties. Man Luo et. al.[30] have prepared one-pot synthesis of CdS and Ni-doped CdS hollow spheres. The optical properties of bulk II-VI semiconductors containing manganese are essentially modified by electronic transitions within the half-filled 3d shell of the Mn^{2+} ions.[31] Doping Mn^{2+} can alter the charge separation and recombination dynamics by creating electronic states in the midgap region, which is in favor of the improvement of power conversion efficiency.[32] Min Yan et. al. have prepared triangular Mn doped CdS nanowires[33] and Chuanwei Cheng et. al. have prepared single-crystal Mn^{2+}-doped CdS nanowires.[34] Mn^{2+} has been the most extensively studied luminescence activator in II–VI semiconductor. Mn doped CdS NPs are interesting because of the fact that Mn^{2+} ions provide good traps for the excited electrons, which gives rise to their potential use in nonlinear optics, electronic and optoelectronic devices. These exciting

achievements motivated us to investigate Mn^{2+} doped CdS hollow spheres. Herein, we report a simple template-free hydrothermal method to prepare Mn-doped CdS hollow spheres using biomolecule L-Glutathione reduced (GSH) as sulfur source and bubble source. A large-scale of uniformed and well dispersed Mn-doped CdS hollow spheres were obtained without traditional tedious and intricate template removal procedures. This one-step route provides both the expected hollow structure and the Mn^{2+} doping. In addition, we experimentally demonstrate the as-prepared Mn-doped CdS hollow spheres have an enhanced photocatalytic activity and improved durability for organic pollutants removal. The possible effect factors for the activity and stability are also discussed in detail.

2. Experiment details

2.1 Materials

Manganese acetate tetrahydrate ($Mn(CH_3COO)_2{\cdot}4H_2O$) was purchased from Sinopharm Chemical Reagent Co, Ltd (Shanghai, China), GSH($C_6H_{12}N_2O_4S_2$) and cadmium nitrate tetrahydrate ($Cd(NO_3)_2{\cdot}4H_2O$) were purchased from Aladdin. All chemicals used in the experiments are of analytical grade and were used without further purification.

2.2 Synthesis of Mn-doped CdS

In a typical preparation, 0.825 mmol of GSH, appropriate molar ratios of $Cd(NO_3)_2{\cdot}$ $4H_2O$ and $Mn(CH_3COO)_2{\cdot}4H_2O$ with the total mole number of Cd^{2+} and Mn^{2+} being 0.825 mmol were dissolved into a mixed solution of 80.0 mL of deionized water. The Mn-doping concentration was designed as 1.0, 2.0, 3.5, and 5.0 mol% (denoted as X mol% Mn-doped CdS), which was the mole ratio of the theoretical yield. After being continuously stirred for 1 h, the clear solution was transferred into a stainless steel vessel (Teflon cups with an inner volume of 100 mL), which was heated and maintained at 180 □ for 5 h and then cooled to room temperature naturally. The products were obtained by suction filtration, washed with de-ionized water and anhydrous ethanol alternately, and then dried at 60 ℃ overnight in an oven. Through varying the molar percentage of Mn^{2+} in the solutions, a series of Mn-doped CdS hollow spheres with different compositions were obtained.

2.3 Characterization

The structure and phase of the samples were characterized by power X-ray diffraction (XRD) employing a scanning rate of 0.05°/S in the 2θ range from 10° to 80°, in a Bruker D8 Advance using monochromatized Cu K_α=1.5404Å. The microstructure and composition size were observed using a

transmission electron microscope (TEM) and high-resolution transmission electron microscopy (HRTEM) using a Tecnai G20 microscope operated at an accelerating voltage of 200 kV with an energy-dispersive X-ray spectrometer (EDS) performed at 300 kV, respectively. The specimens of TEM and HRTEM measurements were prepared by spreading a droplet of ethanol suspension onto copper grids coated with perforated carbon films, and allowed to dry in air. Scanning electron micrographs (SEM) were performed with a SU8000 field-emission scanning electron microscope (FESEM, Hitachi, Japan) at an accelerating voltage of 15 KV. The surface composition of the catalysts was analyzed by X-ray photoelectron spectroscopy (XPS) which was equipped with a VG Multilab 2000 (VG Inc.) photoelectron spectrometer using monochromatic Al K_{α} radiation under vacuum at 2×10^{-6} Pa. All the binding energies were referenced to the C1s peak at 284.8 eV of the surface adventitious carbon. The UV-vis DRS were collected using a Shimadzu UV-2450 spectrophotometer from 200 to 800 nm using $BaSO_4$ as background. Reactive brilliant rhodamine-B (RhB) and methyl orange (MO) were chosen as the simulated pollutants to evaluate the photocatalysis activities of the as-prepared Mn-doped CdS hollow spheres. The catalytic mechanism and durability of the photocatalyst were also discussed.

2.4 Photocatalytic Activities and Durability Measurements

The photocatalytic activity of the sample was evaluated by the degradation of dye RhB (50 mL, 1×10^{-5} mol L^{-1}) and MO (50 mL, 10mg L^{-1}) under simulated visible-light (equipped with a 420 nm cutoff filter) irradiation by a 350 W Xe lamp with 32.86 lm/W luminous efficiency. In each experiment, 50 mg of the photocatalyst and 50 mL of aqueous solution of RhB or MO were added into a flask, the suspension was ultrasonic treatment for 10 min and stirred for 1h in the dark in order to reach the adsorption-desorption equilibrium at room temperature. The reaction was ensured at room temperature and reduce the interference of the infrared radiation by passing into condensate water. At given time intervals, 3 mL liquid were sampled and then filtered to remove the catalyst particles for analysis. The filtrates were finally analyzed using a UV-vis spectrophotometer (UV-2450).

In order to test Mn-doped CdS hollow spheres durability, four cycles of photocatalytic measurements were employed by using 2.0 mol% Mn-doped CdS hollow spheres as a representative sample. The photocatalyst was separated from aqueous solution after each run of reactions. The filtered catalyst was washed by anhydrous ethanol and reused in the subsequent recycling experiment. After the experiment, the XRD spectrum of the final catalyst was also detected.

2. 5 Analysis of Hydroxyl Radicals (·OH)

The formation of ·OH on the surface of the UV and Vis illuminated samples was detected by a photoluminescence (PL) method using coumarin as a probe molecule. Coumarin can readily react with ·OH to produce the highly fluorescent product, 7-hydroxycoumarin (7HC) (umbelliferone).[35] The experimental procedure was similar to the measurement of photocatalytic activity. In a typical process, 2.0 mol% Mn-doped CdS (50 mg) hollow spheres and coumarins (50 mL, 5.0×10^{-4} mol L^{-1}) were ultrasonic treatment for 10 min and magnetic stirring for 1h under dark conditions. Then, the mixture was irradiated under visible-light (λ>420 nm). At given time intervals, 3 mL liquid were sampled and then filtered to remove the catalyst particles for measure the increase in the PL intensity around 445 nm excited by 332 nm light.

3 Results and discussion

3.1 Microstructure characterizations

XRD measurements were employed to investigate the phase and structure of the CdS and Mn-doped CdS samples. As shown in Fig. 1, these samples show the similar line type, and all can be assigned to the hexagonal CdS that with six characteristic diffraction peaks according to the standard JCPDS card (NO. 77-2306). As no signals about manganese or other impurities were detected in these spectra, it can be concluded that the doping of Mn^{2+} has little effect on the crystalline phase of CdS. The possible reason may result from the low dosage of Mn^{2+}. However, with the increasing of Mn^{2+} content in the precursors, the peak intensity of these samples became stronger gradually, suggesting these samples tend to be well crystallized.

The morphology of Mn-Doped CdS hollow spheres microspheres was studied by SEM and TEM. Fig. 2 is the SEM and the TEM images of 2.0 mol% Mn-doped CdS hollow spheres with different magnifications and the corresponding HRTEM Image. Fig. 2(a) shows these microspheres with average diameter of about 300-600 nm, moreover, it is obvious that the surface of the sphere is coarse. From the broken sphere in Fig. 2(b), we can clearly find that the spheres have typical hollow interior structure, it can be further clearly observed that the thickness of the wall of the broken hollow sphere is about 60 nm, indicating the thickness of hollow sphere. In Fig. 2(c), a clear contrast between the dark edge and the pale center can be observed, which confirms that all the spheres have a hollow interior again. The Fig. 2(a)-(c) indicated that these rough shells were constructed of loosely packed fine nanoparticles. These nanoparticles which accumulated the spheres, as building blocks for the spheres,

can produce inherent porosity. Just these inherent aperture create numerous nanoscale channels for chemical moieties travelling between the interior cavity and exterior space, which making the hollow spheres is particularly suitable for further studies in adsorption and catalytic applications.[8] Fig. 2(d) shows the corresponding high resolution TEM image, it shows clear lattice fringes, which allowed for the identification of crystallographic spacing. The corresponding fast Fourier transform (FFT) pattern is shown in the inset of Fig. 2(d). As shown in Fig. 2(d), the crystallographic spacing of the 2.0 mol% Mn-doped CdS hollow spheres estimated from the HRTEM image was about 0.3582, 0.3357 and 0.3160 nm; which respectively corresponding to the (100) (002) and (101) faces. Meanwhile, the lattice spacing of 0.3582, 0.3357 and 0.3160 nm corresponds to the (100), (002) and (101) faces of hexagonal CdS. These results are consistent with the XRD analysis.

Fig. 3 shows the TEM image of Mn-doped CdS with different Mn^{2+} doping concentration. In all images of Fig. 3, the edge of these spheres is darker than their center, which clearly reveals the hollow natural characteristic of these spheres, and indicates that the hollow structures can be generated in different Mn^{2+} doping concentration. No significant difference in the size and thickness of the spheres even the Mn^{2+} concentration increased to 5 mol%, but fewer nanorods appeare in the edge of the spheres. These TEM images show the gradual develop process of the morphology following the increase of the Mn^{2+} concentration.

In an effort to gain further insight into the surface information of the samples, pure CdS, 2.0 and 5.0 mol% Mn-doped CdS samples were investigated by XPS. Because of the low doping concentration, the signals of Mn 2p are very weak and it is hard to be detected. Fig. 4 provides the information of binding energies and intensities of the surface element of S 2p of CdS and 2.0 and 5.0 mol% Mn-doped CdS. Compared with pure CdS, it can be found that the position of the peak shifts to a higher energy as the concentration of Mn^{2+} increases. This may be because that some Cd^{2+} replaced by Mn^{2+} of the CdS lattice and formed Cd-S-Mn bonds in the Mn-doped CdS samples. The difference in electronegativity (χ) between Cd (χ_p = 1.69), S (χ_p = 2.56) and Mn (χ_p = 1.55) results in a higher electron cloud density of S atoms, thus the binding energy of S 2p (161.36 and 161.58 eV for 2.0 and 5.0 mol% Mn-doped CdS respectively) increases compared to pure CdS (161.34 eV). The asymmetric band of S 2p of Mn-doped CdS samples can be fitted into two peaks, the peaks at about 161.09 and 161.30 eV can be assigned to the S atoms bonded to the Cd atoms. Similarly, the peaks at about 162.14 and 162.38 eV which can be assigned to the S atoms bonded to the Mn atoms, are mainly due to the partial substitution of Cd^{2+} by Mn^{2+} in the CdS lattice.

UV-vis diffuse reflectance spectra (DRS) were measured to determine the optical properties of the undoped and Mn-doped CdS hollow spheres. As shows in Fig. 5, all the samples have strong absorption in the visible-light region and these can be assigned to the intrinsic band gap absorption of CdS. The direct band gap values of the undoped and Mn-doped CdS hollow spheres samples were estimated from the $(Ahυ)^2$ versus photon energy (hυ) plot as shown in the insert of the Fig. 5, where A, h and υ is the absorbance value, Planck constant and light frequency, respectively. After comparison, a slight blue shift is observed in the samples doped with Mn. This slight blue shift in the absorption edge is the outcome of the quantum confinement effect. This effect is due to the increasing of nucleation rates with increase in doping concentrations.[36] The band gap of CdS (2.30 eV) is lower than that of all the Mn-doped CdS hollow spheres (2.38, 2.36, 2.32 eV). This indicates that the introduction of Mn^{2+} has a significant effect on the optical property of light absorption for the as-prepared Mn-doped CdS hollow spheres.

3.2 Photocatalytic Properties of Mn-Doped CdS

To demonstrate the potential applicability of Mn-doped CdS hollow spheres, the photocatalytic degradation of dye RhB under visible light irradiation (λ>420 nm) had been chosen as a model reaction to evaluate the photocatalytic activities of the prepared samples (Fig. 6). According to the reference, commercial product Degussa P25 and commercial CdS were also investigated under the same experimental conditions. As can be seen from Fig. 6, only a negligible activity is detected when the catalyst is free. Both of the CdS and Mn-doped CdS hollow spheres are much superior to that of commercial CdS, indicating the advantage of hollow structure. The unique hollow structure of Mn-doped CdS hollow spheres enables both the outer and inner surfaces of the catalyst to contact with RhB molecules and provides more active sites to interact, and allows multiple reflections of visible light within the interior cavities to promote the light-harvesting efficiencyc.[37,38]

It can be found that all the Mn-doped CdS hollow spheres show enhanced activities than that of undoped CdS hollow spheres. It is possible that the Mn^{2+} doping can provide them with intriguing properties inherited from the synergetic effect. While we can find that the activity of Mn-doped CdS hollow spheres is not be enhanced monotonously with the Mn^{2+} content increasing. This can be partly attributed to the relatively high doping concentrations of Mn^{2+}, which might cause a reduced adsorption of RhB and become the recombination center of photogenerated carriers, resulting in a decrease of photocatalytic efficiency.[39]

It is also found that the 2.0 mol% Mn-doped CdS hollow spheres demonstrated highest activity in

the series of Mn-doped CdS photocatalysts. After 25min of visible light irradiation, the RhB removal over is as low as 0.3 % and the degradation ratio of 99.73 %, which indicates that Mn-doped CdS has more higher photocatalytic activity than Ni-doped CdS for RhB degradation.[30] Compare with the reaction rate constants (k), we can find that the RhB removal rate of the 2.0 mol% Mn-doped CdS hollow sphere (k= 0.1915) is about 5 times as much as that of CdS hollow sphere (k=0.0399). Therefore, it is believed that doped right amount of Mn^{2+} contributed to enhanced the activity of CdS hollow sphere. This can be attributed to more efficient light harvesting by special structure and effective separation of photogenerated carries affected by optimal Mn^{2+} doping. Fig. 7 shows the temporal evolution of absorption spectra of an RhB aqueous solution (initial concentration is 1.0×10^{-5} M, 50 mL) in the presence of 50 mg 2.0 mol% Mn-doped CdS hollow spheres under visible light (λ>420 nm) irradiation. After 25 min irradiation, the maximum absorption band of the solution gradually shifted from 553.5 to 496 nm, which indicated that the de-ethylation process instead of the decomposition of the conjugated chromophore structure is the dominant process,[40] and the color of RhB aqueous solution changed from pink to colourless. Meanwhile, the absorption band gradually decreased, which indicated that the ethyl groups of RhB were removed during irradiation[41-43]. For further investigating the photodegradation of RhB, the total organic carbon (TOC) removal in corresponding solutions at different exposure time were detected, as shown in the insert of the Fig. 7. With the extension of irradiation time, the concentration of organic carbon decreased steadily, indicating that RhB dye can not only be discolored but also degraded over Mn-doped CdS. It can be seen that the TOC removal efficiency increases to 52.9% for RhB after 25 min. These results further confirmed that RhB pollutants can be removed efficiently. Cd^{2+} is a toxic pollutant, the content of Cd^{2+} is high in our Mn-doped CdS. However, the release of Cd^{2+} to water only accounted for 0.89 wt% of bulk Mn-doped CdS.

For further testing the high activity of the 2 mol% Mn-doped CdS hollow spheres, MO, a typical chemically stable and difficultly decomposed dye, was also chosen as the goal contaminant to photocatalytic degradation under visible light irradiation (λ>420 nm). Fig. 8 shows the change of absorption spectra of MO aqueous solution in the presence of 50 mg catalyst. It can be seen that the decomposition of organic pollutants MO is efficient and the degradation ratio of 99.2 % after 50 min, which indicated that the 2.0 mol% Mn-doped CdS hollow spheres shows a relatively high photocatalytic performance. To further demonstrate the brilliant photocatalytic activity of 2 mol% Mn-doped CdS hollow spheres, salicylic acid, a typical colorless pollutant which has no light

adsorption in the visible light region was also chosen as the goal contaminant. Figure 9 shows the UV-vis spectra of salicylic acid versus reaction time, in 4 h irradiation of visible light, salicylic acid almost can be completely degraded, the result demonstrated again the high activity of our Mn-doped CdS.

In order to test the stability of the Mn-doped CdS hollow spheres, we reused the catalyst for four recycles by RhB degradation under visible light (λ>420 nm) irradiation. As shown in Fig. 10, the catalyst could be reused four times without significant deactivation after 4 times recycling, the stability of the Mn-doped CdS hollow spheres is similar to Ni-doped CdS hollow spheres.[30] The corresponding XRD patterns (Fig. 11) have no notable peak shift before and after the photocatalytic recycles except for a slightly enhanced intensity in diffraction peaks, indicating the high stability of the Mn-doped CdS hollow spheres.

It is well known that the hydroxyl radical (·OH) is one of the major active species responsible for the photodegradation of organic molecules in the photcatalytic process.[44] In order to further insight into the photocatalytic mechanism and study the active species involved in the photocatalytic process, the PL technique was employed to detect hydroxyl radicals (·OH) on the surface of visible light illuminated Mn-Doped CdS spheres by using coumarin as a proble molecule.[35] Fig. 12 shows the changes in the PL spectra for 5.0×10^{-4} M coumarin solution with irradiation time in the presence of the 2.0 mol% Mn-Doped hollow spheres. A gradual increase in the PL intensity at about 445 nm is observed with increasing irradiation time indicating the production of ·OH radicals. However, no increased PL intensity is observed in the absence of light irradiation or Mn-Doped CdS hollow spheres, which confirms that the fluorescence is caused by chemical reactions of coumarin with ·OH formed at the Mn-doped CdS hollow spheres-water interface via a photocatalytic reaction.[45] Therefore, Form this results, we believe that the fast production and the highly accumulated of ·OH radicals may be the main active oxygen species in the photocatalytic process with the Mn-doped CdS hollow sphere system.

4 Conclusions

In summary, by varying the molar ratio of different precursors, we have successfully synthesized a series of Mn-doped CdS hollow spheres with the assistance of GSH act as the S source and a gas bubble-template via a simple hydrothermal method. All the catalysts showed higher photocatalytic activity for the degradation of RhB than commercial Degussa P25 under visible light irradiation. Among the samples, the 2.0 mol% Mn-doped CdS hollow spheres show the highest photocatalytic

activity, and PL spectra demonstrated that ·OH radicals may be the main active oxygen species in the photocatalytic process. The high photocatalytic activity can have a close relationship with the hollow structure as well as the Mn^{2+} doping. The hollow structure may favors for the harvesting of exciting light and facilitates the transportation of reactants and products within the interior space. The doped Mn^{2+} plays a key role in reducing the recombination rate of photon-generated carriers, thus promoted the activity and stability of the catalyst. The method and idea described herein will provide a new way to synthesize not only Mn-doped CdS hollow spheres, but also for other semiconductor materials.

AUTHOR INFORMATION

Corresponding Author

*Tel: +86 27 67841302. E-mail: junchenghuhu@hotmail.com.

Notes

The authors declare no competing financial interest.

ACKNOWLEDGMENTS

This work was supported by Natural Science Foundation of Hubei Province (2013CFA089).

References

1 Y. K. Lai, J. Y. Huang, H. F. Zhang, V. P. Subramaniam, Y. X. Tang, D. G. Gong, L. Sundar, L. Sun, Z. Chen, and C. J. Lin, J. Hazard, *Mater.,* 2010, **184,** 855-863.

2 X. H. Tang and D. Y. Li, *J. Phys. Chem. C,* 2008, **112,** 5405-5409.

3 P. Roy, S. Berger, P. Schmuki, *Angew. Chem. Int. Ed.,* 2011, **50,** 2904-2939.

4 S. W. Liu, J. G. Yu, M. Jaroniec, *J. Am. Chem. Soc.,* 2010, **132,** 11914-11916.

5 X. H. Li, J. S. Zhang, X. F. Chen, A. Fischer, A. Thomas, M. Antonietti, X. C. Wang, *Chem. Mater.,* 2011, **23,** 4344-4348.

6 M. Ibáñez, J. D. Fan, W. H. Li, D. Cadavid, R. Nafria, A. Carrete, and A. Cabot, *Chem. Mater.,* 2011, **23,** 3095-3104.

7 Z. Y. Liu, H. W. Bai, D. Sun, *Appl. Catal. B: Environ.,* 2011, **104,** 234-238.

8 M. Luo, Y. Liu, J. C. Hu, J. L. Li, J. Liu, R. M. Richards, *Appl. Catal. B: Environ.,* 2012, **125,** 180-188.

9 Y. Ishibai, J. Sato, T. Nishikawa, S. Miyagishi, *Appl. Catal. B: Environ.,* 2008, **79,** 117-121.

10 Y. Liu, L. F. Chen, J. C. Hu, J. L. Li, R. Richards, *J. Phys. Chem. C,* 2010, **114,** 1641-1645.

11 Y. Liu, J. C. Hu, J. L. Li, *Journal of Alloys & Compounds,* 2011, **509,** 5152-5158.

12 X. Chen, L. Liu, P. Y. Yu, S. S. Mao, *Science,* 2011, **331,** 746-750.

13 Y. J. Xu, Y. B. Zhuang, X. Z. Fu, *J. Phys. Chem. C,* 2010, **114,** 2669-2676.

14 M. F. Wu, Y. N. Jin, G. H. Zhao, M. F. Li, D. M. Li, *Environ. Sci. Technol.,* 2010, **44,** 1780-1785.

15 K. L. Lv, Q. J. Xiang, J. G. Yu, *Appl. Catal. B: Environ.,* 2010, **104,** 275-281.

16 D. J. Wang, D. S. Li, G. Li, F. Fu, Z. P. Zhan, Q. T. Wei, *J. Phys. Chem. C,* 2009, **113,** 5984-5990.

17 G. Z. Shen, C. J. Lee, *Crystal Growth & Design,* 2005, **5,** 1085-1089.

18 J. Zhang, S. W. Liu, J. G. Yu, M. Jaroniec, *J. Mater. Chem.,* 2011, **21,** 14655-14662.

19 A. P. Davis, C. P. Huang, *Water. Res.*, 1991, **25,** 1273-1278.

20 F. Chen, R. J. Zhou, L. G. Yang, N. Liu, M. Wang, H. Z. Chen, *J. Phys. Chem. C,* 2008, **112,** 1001-1007.

21 X. Zong, G. P. Wu, H. J. Yan, G. J. Ma, J. Y. Shi, F. Y. Wen, L. Wang, C. Li, *J. Phys. Chem. C,* 2010, **114,** 1963-1968.

22 G. S. Li, D. Q. Zhang, J. C. Yu, *Environ. Sci. Technol.,* 2009, **43,** 7079-7085.

23 T. Gao, T. H. Wang, *Chem. Commun.,* 2004, **22,** 2558-2559.

24 J. Choi, S. Y. Ryu, W. Balcerski, T. K. Lee, M. R. Hoffmann, *J. Mater. Chem.,* 2008, **18,** 2371-2378.

25 X. J. Lv, F. Q. Huang, X. L. Mou, Y. M. Wang, F. F. Xu, *Adv. Mater.,* 2010, **22,** 3719-3722.

26 S. L. Xiong, X. G. Zhang, Y. T. Qian, *Cryst. Growth Des.,* 2009, **9,** 5259-5265.

27 T. Shanmugapriya, R. Vinayakan, K. G. Thomas, P. Ramamurthy, *Cryst. Eng. Comm.,* 2011, **13,** 2340-2345.

28 Y. Shemesh, J. E. Macdonald, G. Menagen, U. Banin, *Angew. Chem. Int. Ed*., 2011, **50,** 1185-1189.

29 J. X. Li, J. H. Xu, W. L. Dai, H. X. Li, K. N. Fan, *Appl. Catal. B: Environ.,* 2009, **85,** 162-170.

30 M. Luo, Y. Liu, J. C. Hu, H. Liu, J. L. Li, *Appl. Mater. & Interfaces,* 2012, **4,** 1813-1821.

31 O. Goede and W. Heimbrodt, *Phys. Status Solidi,* 1988, **146**, 11-62.

32 L. B. Yu, Z. Li, Y. B. Liu, F. Cheng, S. Q. Sun. Mn-doped CdS quantum dots sensitized hierarchical TiO_2 flower-rod for solar cell applicationthe, *Applied Surface Science*, 2014, **305**, 359-365.

33 M. Yan, G. Z. Dai, S. Hu, Q. L. Zhang, B. S. Zou, *Mater. Letters,* 2011, **65,** 2522-2525.

34 C. W. Cheng, G. Y. Xu, H. Q. Zhang, H. Wang, J. M. Cao, H. M. Ji, *Mater. Chem. and Phy.,* 2006, **97,** 448-451.

35 Y. Liu, J. C. Hu, T. F. Zhou, R. C. Che, J. l. Li, *J. Mater. Chem.,* 2011, **21,** 16621-16627.

36 D. Anshu, P. Vijay, S. Kuldeep, Rathore, *Cataly. Commun.,* 2012, **28,** 90-94.

37 Y. N. Huo, M. Miao, Y. Zhang, J. Zhu, H. X. Li, *Chem. Commun.,* 2011, **47,** 2089-2091.

38 X. W. Lou, L. A. Archer, Z. C. Yang, *Adv. Mater.,* 2008, **20,** 3987-4019.

39 X. H. Zhang, D. W. Jing, L. J. Guo, *Int. J. Hydrogen Energy,* 2010, **35,** 7051-7057.

40 W. Zhao, C. Chen, X. Li, J. Zhao, Photodegradation of sulorhodamine-B dye in platinum as a functional co-catalyst, *J. Phys. Chem. B*, 2002, **106**, 5022-5028.

41 N. U. Silvaa, T. G. Nunesb, M. S. Saraiva, M. S. Shalamzari, P. D. Vaz, O. C. Monteiroa, C. D. Nunes, *Appl. Catal. B: Environ.,* 2012, **113-114,** 180-191.

42 D. Chen, J. H. Ye, *Adv. Funct. Mater.,* 2008, **18,** 1922-1928.

43 H. B. Fu, C. S. Pan, W. Q. Yao, Y. F. Zhu, *J. Phys. Chem. B,* 2005, **109,** 22432-22439.

44 T. Hirakawa, K. Yawata, Y. Nosaka, *Appl. Catal. A:General,* 2007, **325,** 105-111.

45 C. S. Turch, D. F. Ollis, *Journal of Cataly.,* 1990, **122,** 178-192.

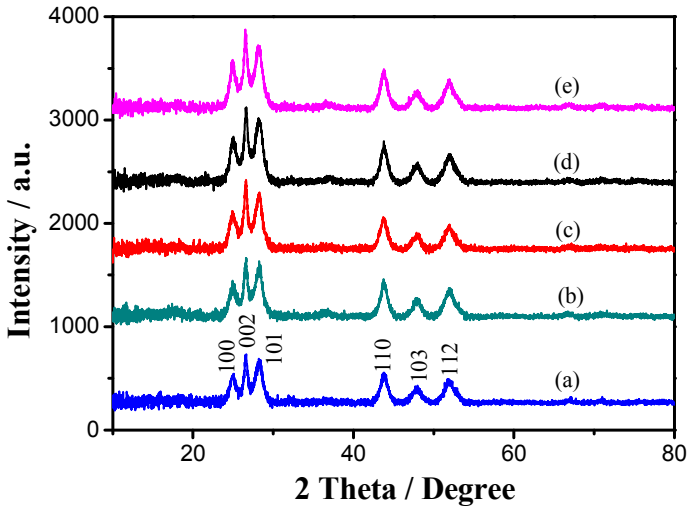

Fig. 1. XRD patterns of (a) CdS, (b) 1.0 mol % Mn-doped CdS, (c) 2.0 mol % Mn-doped CdS, (d) 3.5 mol % Mn-doped CdS, (e)5.0 mol % Mn-doped CdS.

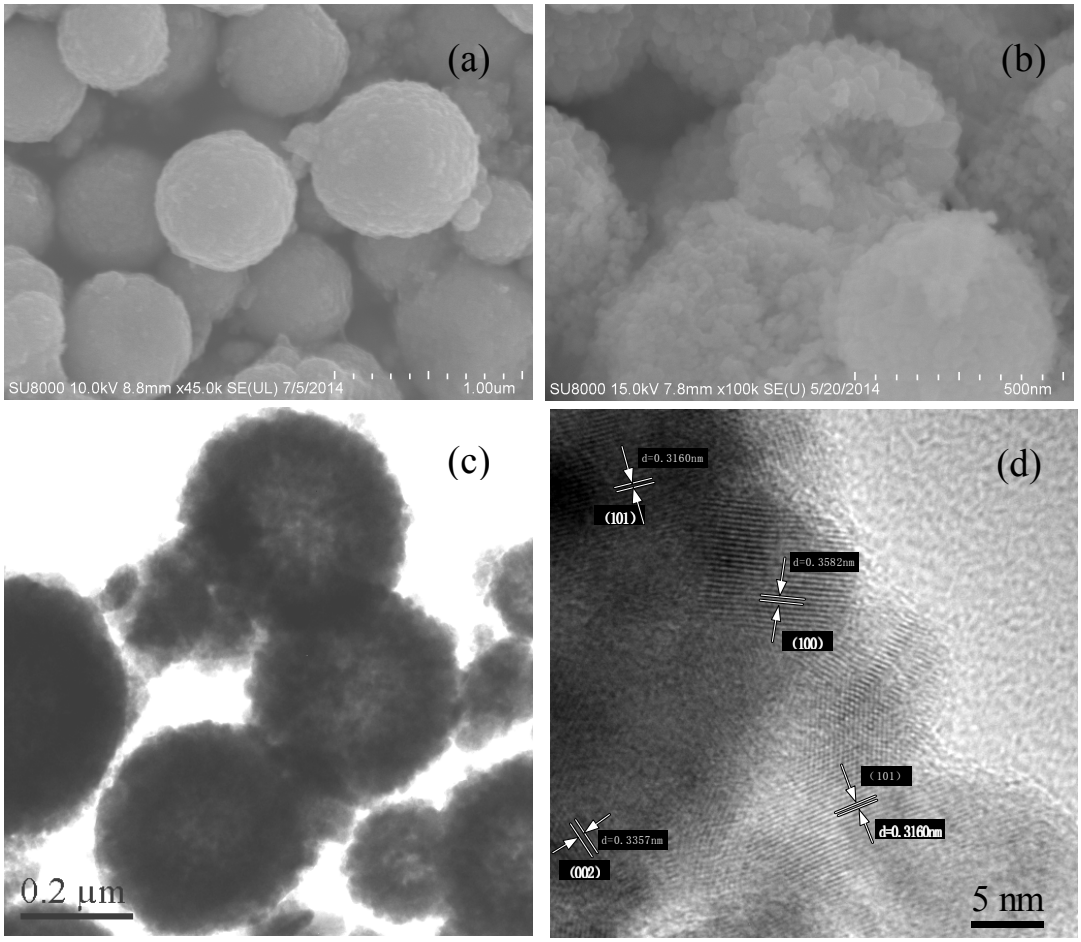

Fig. 2. (a) and (b) are SEM images of 2.0 mol % Mn-doped CdS, (c) is TEM image and (d) is the corresponding HRTEM image.

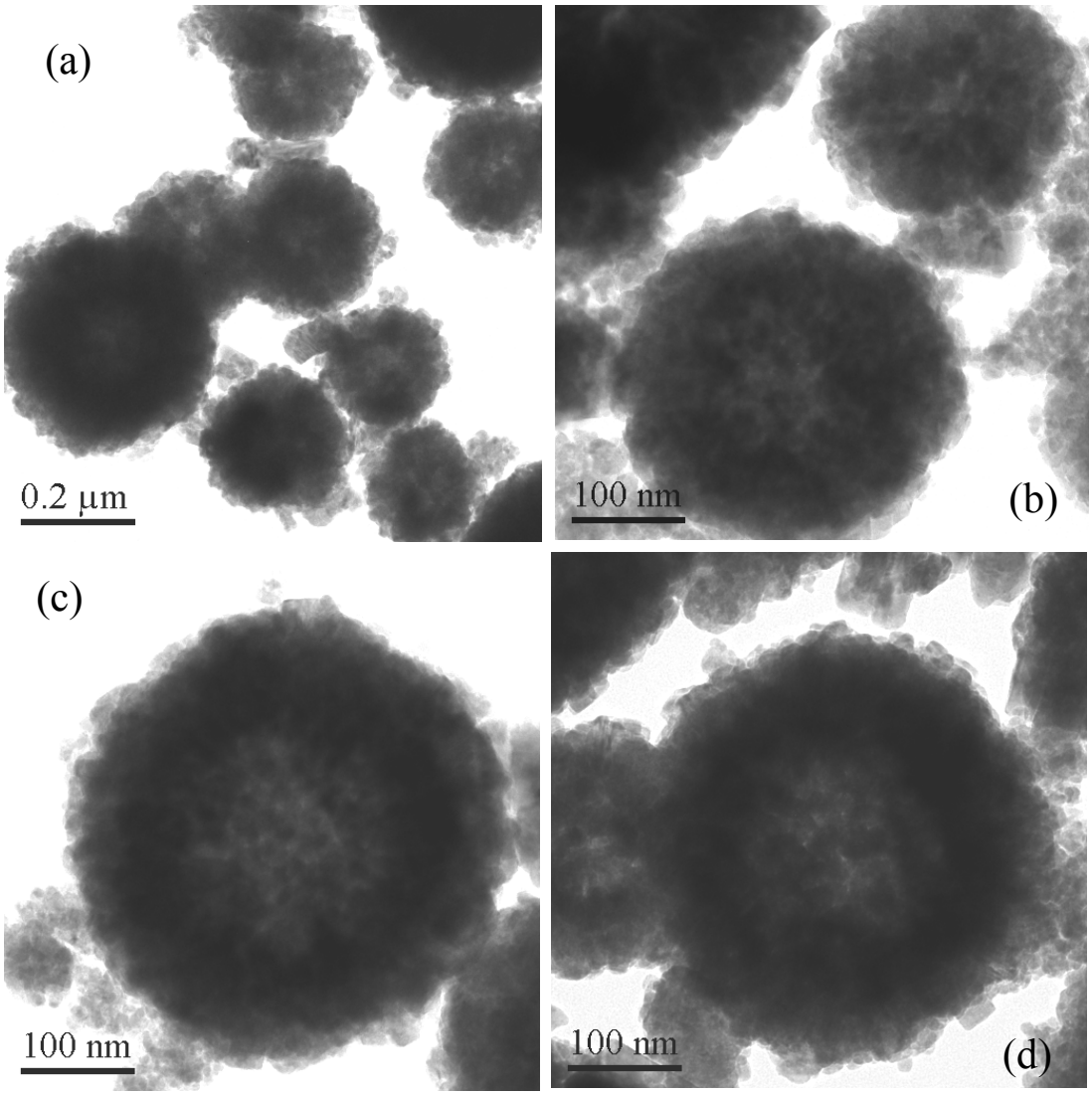

Fig. 3. TEM image of (a) CdS, (b) 1.0 mol % Mn-doped CdS, (c) 3.5 mol % Mn-doped CdS and (d) 5 mol % Mn-doped CdS.

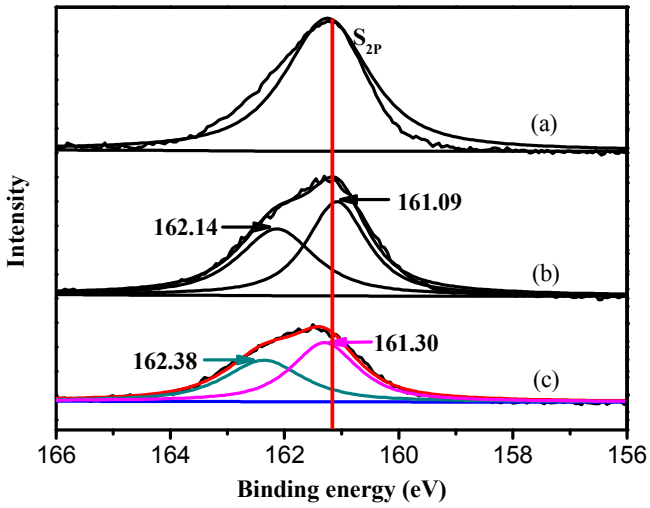

Fig. 4. XPS results of S 2p of (a) CdS, (b) 2.0 mol %, and (c) 5.0 mol % Mn-doped CdS.

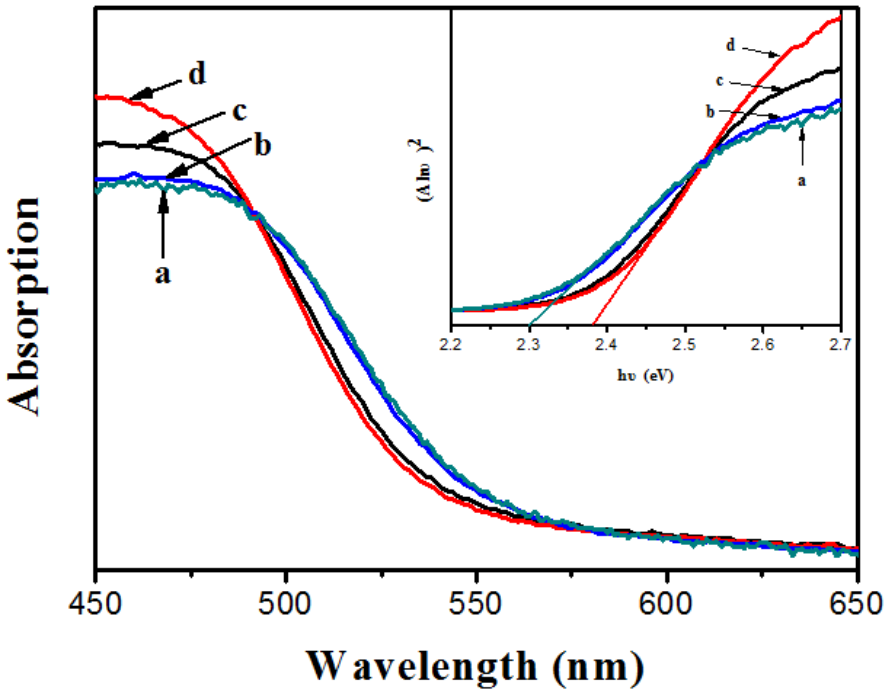

Fig. 5. UV−vis DRS of (a) CdS, (b) 2.0 mol % Mn-doped CdS, (c) 1.0 mol % Mn-doped CdS, and (d) 3.5 mol % Mn-doped CdS . The inset is band gap evaluation from the plots of $(Ah\upsilon)^2$ versus photon energy ($h\upsilon$).

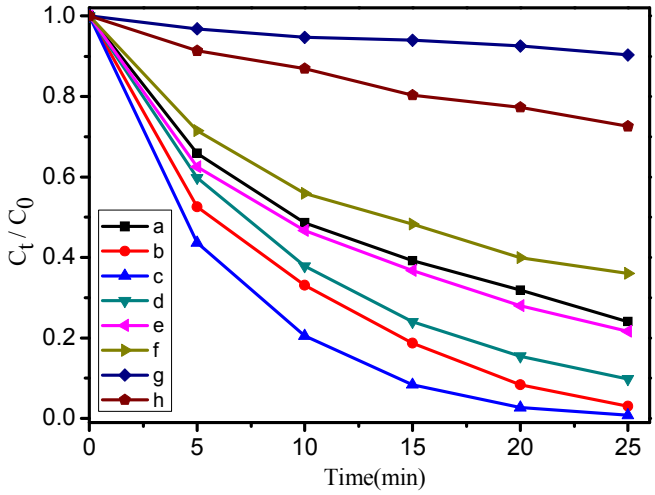

Fig. 6. Photocatalytic degradation curves of RhB under visible light (λ >420 nm) irradiation over (a) CdS hollow spheres, (b) 1.0 mol % Mn-doped CdS, (c) 2.0 mol % Mn-doped CdS, (d) 3.5 mol % Mn-doped CdS, (e)5.0 mol % Mn-doped CdS, (f) Degussa P25, (g). catalyst-free, (h) commercial CdS

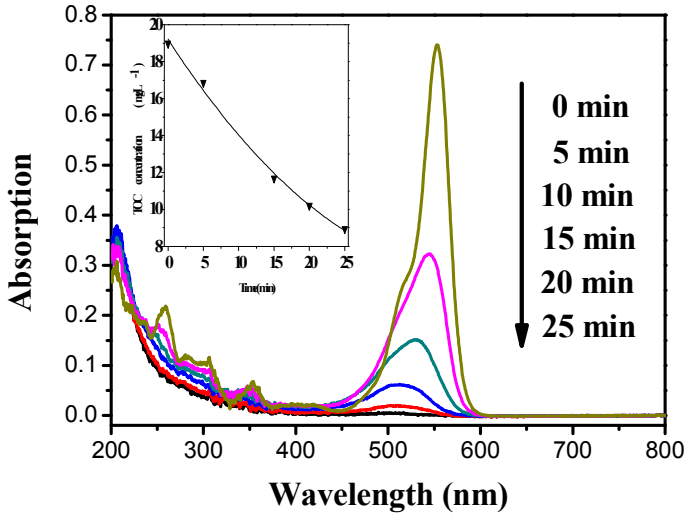

Fig. 7. The absorption spectra of a solution of RhB (1.0×10^{-5} M, 50 mL) in the presence of 2.0 mol % Mn-doped CdS (50mg) under visible light (λ >420 nm) irradiation.

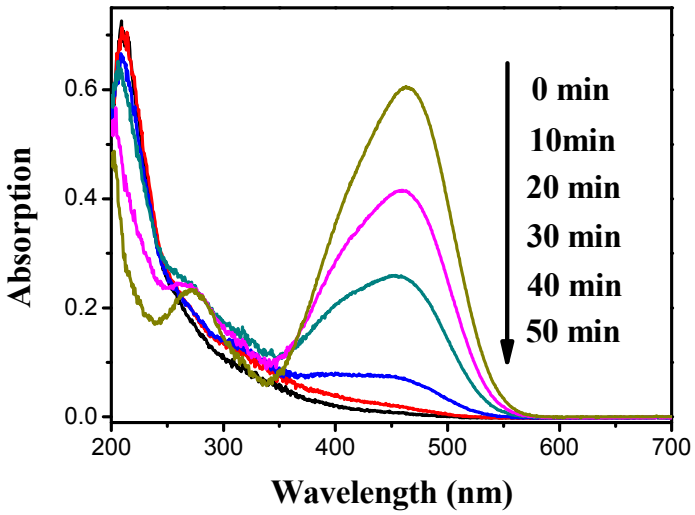

Fig. 8. The absorption spectra of a solution of MO (10 mg / mL, 50 mL) in the presence of 2.0 mol % Mn-doped CdS (50 mg) hollow spheres under visible light ($\lambda > 420$ nm) irradiation.

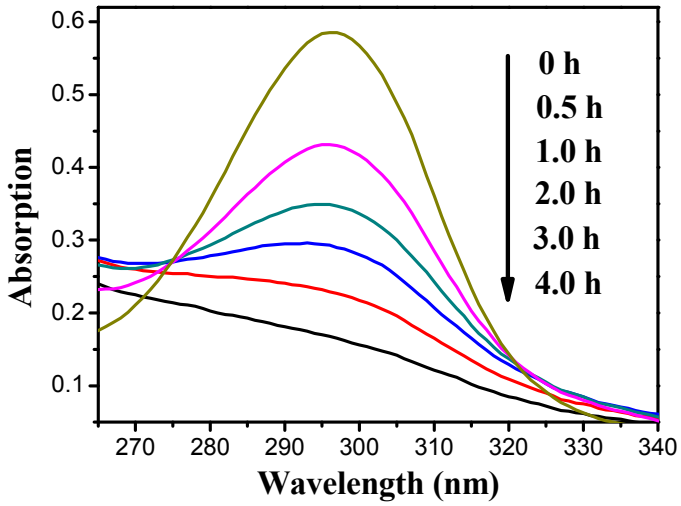

Fig. 9. The absorption spectrum of a solution of salicylic acid (20 mgL^{-1}, 50 mL) in the presence of 2.0 mol% Mn-doped CdS (50 mg) under visible light(>420 nm) irradiation.

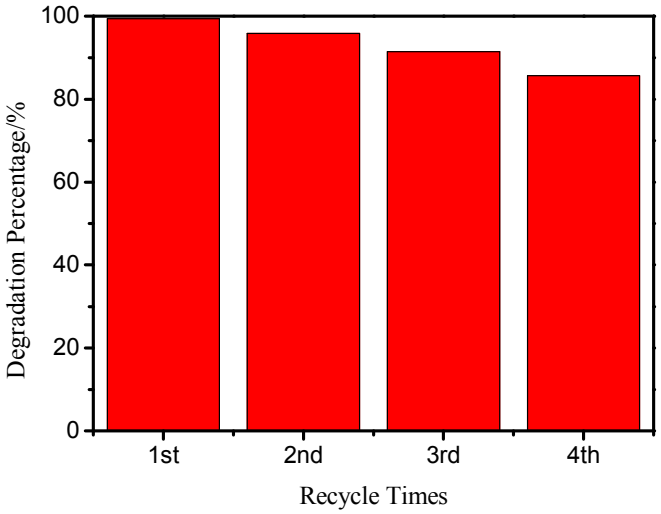

Fig. 10. Recycled photodegradation of RhB under the visible light (> 420 nm) irradiation over 2.0 mol % Mn-doped CdS hollow spheres.

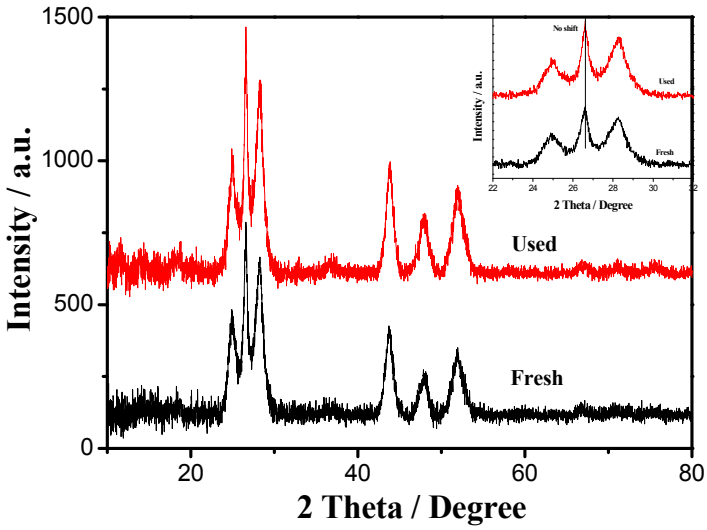

Fig. 11. XRD patterns of 2.0 mol % Mn-doped CdS before and after being used for fourth times.

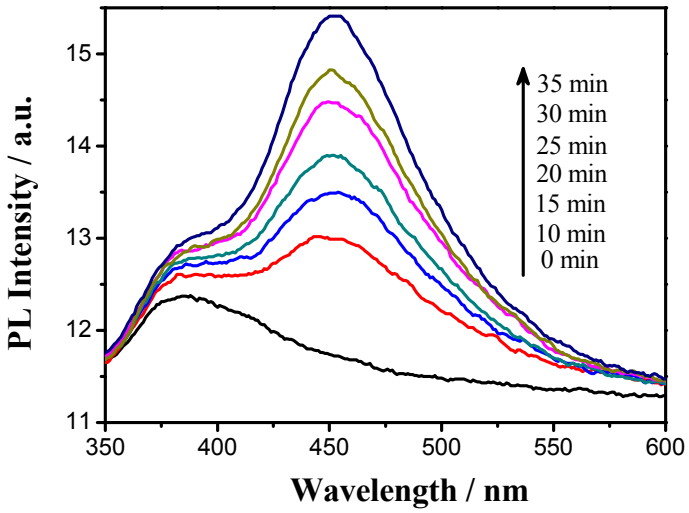

Fig. 12. PL spectra changes observed during visible light illumination (>420 nm) of 2.0 mol % Mn-doped CdS hollow spheres in 5×10^{-4} M coumarin solution (excitation at 332 nm).